Isı Bilimi ve Tekniği Dergisi, 40, 1, 167-175, 2020
J. of Thermal Science and Technology

ISSN 1300-3615

RADIOFREQUENCY ABLATION FOR SPHERICALLY-SHAPED HEPATIC TUMORS

Güven Hasret YILMAZ*, Uğur Tuna YAY*, Oğuz TURGUT*, Burak TIĞLI* and Nuri Eren TÜRKOĞLU**
*Gazi University, Faculty of Engineering, Department of Mechanical Engineering
06570 Maltepe, Ankara, Turkey
gvn_yilmaz_06@hotmail.com, tuna2706@gmail.com, oturgut2006@gmail.com, buraktigli@gmail.com
**Politecnico di Milano, Department of Electrical Engineering
Milano, Italy, erenturkoglu12@gmail.com

(Geliş Tarihi: 04.04.2019, Kabul Tarihi: 06.03.2020)

Abstract: The purpose of this study is to destroy spherical shape hepatic tumors using radiofrequency ablation method. Three-dimensional finite elements method has been employed. Five different radiofrequency probes for liver tissue have been used to create a spherical-shaped lesion. Investigated parameters are the electrical voltage, ablation time, geometry and number of electrodes. Results have been given as lesion volume and temperature distribution. Results have been compared with the literature results, and it is seen that present results are in good agreement with the literature results. Results show that a spherical shape hepatic tumor can be destroyed using a hybrid electrode construction consisting of four Christmas-tree and four umbrella-shaped electrodes. It is seen that approximately 20 mm-diameter of lesion can be destroyed using hybrid electrode design after eight minutes. It is hoped that hybrid electrode configuration can be used for treatment of spherical shape hepatic tumors in clinical applications.
Keywords: Electrode, Hepatic tumors, Lesion, Radiofrequency ablation

KÜRESEL ŞEKİLLİ KARACİĞER TÜMÖRLERİ İÇİN RADYOFREKANS ABLASYONU

Özet: Bu çalışmanın amacı radyofrekans ablasyon metodunu kullanarak küresel şekilli karaciğer tümörlerinin yok edilmesidir. Üç boyutlu sonlu elemanlar metodu kullanılmıştır. Karaciğer dokusu için beş farklı radyofrekans prop küresel şekilli lezyonu oluşturmak için kullanılmıştır. İncelenen parametreler elektrik voltajı, ablasyon süresi, geometri ve elektrot sayısıdır. Sonuçlar lezyon hacmi ve sıcaklık dağılımı olarak verilmiştir. Sonuçlar literatür sonuçları ile kıyaslanmış ve sonuçların literatür sonuçları ile uyum içinde olduğu görülmüştür. Sonuçlar bir küresel şekilli karaciğer tümörünün dört elektrotlu yılbaşı ağacı tipi ve dört elektrotlu şemsiye-tipi elektrotlardan oluşan hibrit bir elektrot konstrüksiyonuyla yok edilebileceğini göstermiştir. Yaklaşık 20 mm çapındaki bir lezyonun sekiz dakika sonunda hibrit elektrot dizaynı ile yok edilebildiği görülmüştür. Hibrit elektrot konfigürasyonunun klinik uygulamalarda küresel şekilli karaciğer tümörlerinin tedavisi için kullanılması umulmaktadır.
Anahtar Kelimeler: Elektrot, Karaciğer tümörleri, Lezyon, Radyofrekans ablasyonu

NOMENCLATURE

c	Specific heat [kJ/kg K]
c_{bl}	Specific heat of the blood [kJ/kg K]
D	Diameter of the trocar tip [mm]
E	Electric field intensity [V/m]
H	Height of the trocar [mm]
J	Current density [A/m^2]
k	Thermal conductivity [W/m K]
h_{bl}	Heat transfer coefficient of the blood [W/m^3 K]
r	Minor radius [mm]
R	Major radius [mm]
Q_m	Energy generated by the metabolic process [W/m^3]
T	Temperature [K]
T_{bl}	Temperature of the blood [K]
t	Time [s]
ρ	Density [kg/m^3]
ρ_{bl}	Density of the blood [kg/m^3]
σ	Electrical conductivity [S/m]
ω_{bl}	Blood perfusion rate [1/s]

INTRODUCTION

Percutaneous hyperthermia treatments generated with radiofrequency needle electrodes have gained wide popularity in last decades. Primary and secondary tumors could be terminated with no serious complications (Rossi et al., 1998). Also, rehabilitation rates have been increased by the improvement of imaging techniques (Verslype et al., 2012).

Hepatocellular carcinoma (HCC) is the most common primary hepatic tumor in the world (Ferenci et al.,

2010), and the global percentage of HCC increases (Poon et al., 2009). Surgical resection, liver transplantation, and radiofrequency ablation (RFA) treatments are recommended for HCC (Clinical Practice Guidelines, 2012a, 2012b).

RFA is applied primarily to patients instead of surgical resection for unresectable HCC by means of minimally invasive procedure along with highly sensitive necrosis, especially for small HCC (Lin and Lin, 2003). RFA also needs shorter hospitalization, and it has lower complication rates than surgical resection (Ozbek et al., 2016). Some investigators believe that RFA can be used as first option against HCC (Mazzaferro et al., 2009).

RFA has been used first in 1990s and dissipated over in clinics (Livraghi et al., 1999). RFA is applied to 30–40% of HCC patients in Europe and the USA (Clinical Practice Guidelines, 2012a, 2012b). RFA method uses alternative current usually at about 450 kHz-550 kHz to create heat, delivered through a thin instrument known as a probe, to terminate malignant lesions (Chang and Nguyen, 2004; Barajas et al., 2018). Imaging procedures like computed tomography scan, ultrasound or magnetic resonance imaging are used to help guide the probe while the probe enters into the area of the tumor. Depletion of the cells occurs when the temperature reaches about 45ºC-50ºC (Goldberg et al., 1996; Tungjitkusolmun et al., 2002; Haemmerich et al., 2003a). Guidance of imaging procedures and choice of an appropriate probe are important for successful ablation (Tatli et al., 2012).

In probe designs, there are some parameters such as probe tip temperature, impedance, power output etc. to control the ablation action (Ito et al., 2014).

Stippel et al. (2004) stated that about 60% of tumors encountered in liver tissue are in spherical shape. Literature review has showed that RFA method for liver tumors has been investigated by a number of researchers for different electrode types. Tungjitkusolmun et al. (2002) carried out a study to investigate the three-dimensional finite element analysis for radiofrequency hepatic tumor ablation using four-array umbrella-typed electrode. Haemmerich et al. (2003a) evaluated the effect of different cooling water temperatures on lesion size with cooled-tip electrode. Ito et al. (2014) developed a new expandable bipolar device to get wider coagulation volume. De Baere et al. (2001) experimentally studied the radiofrequency liver ablation for two different types of RFA devices with four-array expandable needle electrode and a triple-cluster cooled-tip needle electrode. McGahan et al. (1990) investigated the RFA method with ultrasound guide for plane electrodes. Rossi et al. (1990) concluded that small tumors whose diameters are less than 20 mm could be destroyed by RFA method using linear needles. Curley et al. (1997) studied the bipolar RFA in pig livers. Livraghi et al. (1997) studied saline-enhanced RFA with a single radiofrequency electrode. Lencioni et al. (1998) evaluated feasibility, safety and effectiveness of RFA by using cooled-tip electrode needle in hepatic tumors. Hansen et al. (1999) showed that how local vasculature affects the size and shape of a lesion. Haemmerich et al. (2003b) examined the performance of monopolar and bipolar probes for treating lesions. Lee et al. (2004) studied the saline-enhanced hepatic RFA with dual probe bipolar, monopolar and single probe bipolar modes. Mulier et al. (2005) proposed an updated terminology for the electrodes and multiple electrode systems used in radiofrequency processes. Chen et al. (2009) conducted a study to optimize electrode placement for nine tines for the tumor of liver with and without vessel. Yang et al. (2010) presented a robotic system for large tumor lesions using overlapping ablations. Audigier et al. (2015) carried out a study to model heat propagation in liver with blood vessel using RFA for multi-tine electrode. Kilic et al. (2015) stated that tumor needle track seeding may occur after RFA for hepatic tumor. Therefore, they suggested performing prophylactic needle track coagulation. Cartier et al. (2016) compared monopolar and multipolar probes. Ahmad (2016) conducted a study for the comparison of monopolar cluster and multipolar electrode systems to treat HCC bigger than 25 mm. Choi et al. (2016) conducted a study to analyze the outcomes of multi-channel switching RFA using a separable cluster electrode in patients with HCC. A probabilistic bio-heating finite element model was proposed by Duan et al. (2016) to predict RFA lesions in liver using RFA probe. The effect of nanoparticle injected into tissue with blood vessels on RFA treatment of liver tumor was investigated by Shao et al. (2017) using RFA probe. Their results showed that using nanoparticles increases ablation efficiency. Givehchi et al. (2018) simulated the liver tumor ablation using radiofrequency ablation.

Literature study showed that the electrodes used in literature do not give realistic sphere lesion. Thus, in this study, RFA method for liver tumors with spherically-shaped has been investigated numerically. Investigated parameters are the electrical voltage, ablation time, geometry, and number of electrodes. Simulations are conducted for three, four, six, and two different types of eight electrodes. A hybrid electrode which creates spherical shape is proposed.

MATERIALS AND METHODS

Simulation of percutaneous treatment has been carried out by using a computer (with 16 GB of RAM and 1 TB of total disk space). Finite element method is used for numerical study. Figure 1 demonstrates the design which is used for analyses. Outer cylinder shows the liver tissue which is hosting the probe. When the probe reaches the tumor location, tines deploy through the tissue. After that, generator utilizes the radiofrequency waves from the probe to the ground pads which are resting on the patient thighs. Probe consisting of electrodes, trocar tip, and trocar base is also seen in Figure 1. Trocar tip and electrodes are made of different materials due to necessity of different thermal conductivity values. Big part of the heating/ablation

process is performed by electrodes where the trocar tip is auxiliary component for this process. Adjustable trocar base is made of polyurethane which does not allow the heat flow.

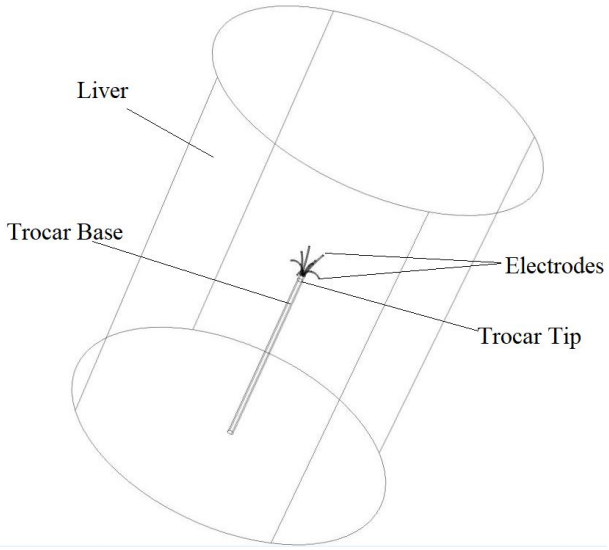

Figure 1. The schematic view of the computational domain.

The five different radiofrequency electrode types used in this study are shown in Figure 2. The electrodes of Case 1 through Case 4 are the Christmas-tree-shaped whereas the electrode given in Case 5 has four Christmas-tree and four umbrella-shaped electrodes. For Case 5, four of eight Christmas-tree-shaped electrodes of Case 4 are changed with four umbrella-shaped electrodes. Thus, the electrode of Case 5 is called as hybrid. The dimensions of electrodes of Case 5 are shown in Figure 3. In Figure 3, r_1 and r_2 are the minor radii. R_1 and R_2 are the major radii. H_1 and H_2 are the heights of trocar tip and Christmas-tree-shaped electrode, respectively. D is the diameter of the trocar tip. The values of these parameters are: r_1=0.23 mm, r_2=0.2 mm, R_1=25 mm, R_2=2.75 mm, H_1=2 mm, H_2=7.962 mm, D=1.8288 mm. The values given in Figure 3 are valid for Case 1 through Case 4. Revolution angle for umbrella-shaped electrodes is 135º. This angle is the most appropriate selection that gives the spherical shape in the best way. However, revolution angle for umbrella-shaped electrodes used in clinical applications is generally 180°. Also, Christmas-tree-shaped electrodes are turned 20° from the vertical axis. There are four main different regions in simulation. These are electrode, trocar tip, tissue, and trocar base. The density ρ (kg/m^3), specific heat c (J/kg K), thermal conductivity k (W/m K), and electric conductivity σ (S/m) of materials of these regions are given in Table 1.

The electrical voltage is chosen between 20-35V. Complete spherical shape is not obtained when electrical voltage is chosen under 30V. In addition, carbonization is observed when electrical voltage is greater than 30V. Thus, 30V is chosen as electrical voltage in this study. The other important values used in the simulation are given in Table 2.

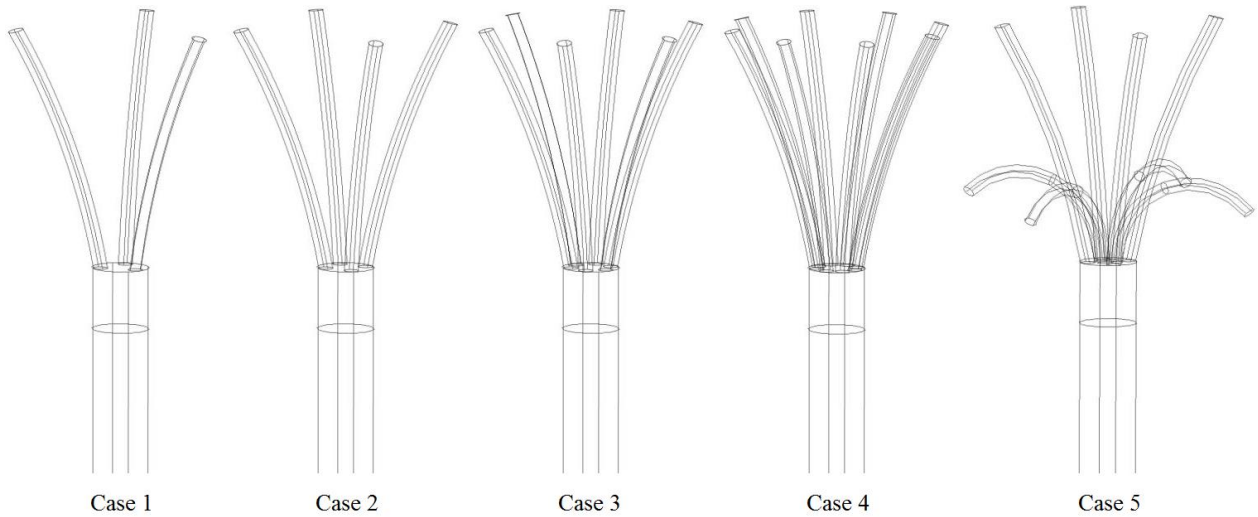

Figure 2. Electrode designs used in this study: Case 1: three-tin, Case 2: four-tin, Case 3: six-tin, Case 4: eight-tin, Case 5: eight-tin (hybrid design).

Table 1. Properties of materials.

Region	Material	ρ (kg/m^3)	c (J/kg K)	k (W/m K)	σ (S/m)
Electrode	Ni-Ti	6450	840	18	10^8
Trocar tip	Stainless steel	21500	132	71	4×10^6
Tissue	Liver	1060	3600	0.512	0.333
Trocar base	Polyurethane	70	1045	0.026	10^{-5}

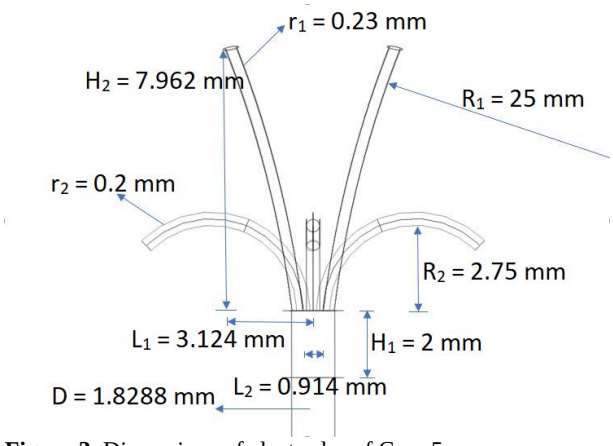

Figure 3. Dimensions of electrodes of Case 5.

Table 2. Parameters used in simulation.

Parameters	Value	Unit
Blood perfusion rate	6.4 x 10^{-3}	1/s
Arterial blood temperature	37	°C
Initial and boundary temperature	37	°C
Electrical voltage	30	V
Ablation time	8	min

Bioheat Equation

Pennes' bioheat equation is a well-known equation and one of the best approaches to simulate RFA in the area of bioheat transfer. Bioheat transfer in radiofrequency tumor ablation occurs between radiofrequency electrode and liver tissue. This type of heating due to electric current flow is called Joule heating. Pennes bioheat transfer equation is given as

$$\rho c\frac{\partial T}{\partial t} = \nabla \cdot k\nabla T + J \cdot E - h_{bl}\left(T - T_{bl}\right) + Q_m \qquad (1)$$

where ρ is the density (kg/m^3), c is the specific heat (J/kg K), k is the thermal conductivity (W/m K), T is the temperature (K), and t is the time (s). J is the current density (A/m^2), E is the electric field intensity (V/m), h_{bl} is the convective heat transfer coefficient (W/m^3 K), and Q_m is the energy generated by the metabolic processes (W/m^3). The convective heat transfer coefficient is given as

$$h_{bl} = \rho_{bl} c_{bl} w_{bl} \qquad (2)$$

In Eq.1 and Eq.2, the subscript *bl* designates the blood, and ω_{bl} is the blood perfusion rate (1/s). Pennes' bioheat equation is solved using finite element method for the cases. COMSOL Multiphysics software is used to solve numerically the governing differential equation, i.e. Eq. 1.

Numerical Analysis

COMSOL Multiphysics software is used to simulate the process. It solves the partial differential equations in an integral form. Unknowns are discretized as sums of basis functions defined on finite elements. To perform an accurate simulation of RFA, different mesh numbers have been used. Tetrahedral mesh (cell) has been employed. Fine mesh structure is employed near the probe. Typical three-dimensional mesh distribution is seen in Figure 4a. Mesh optimization study is carried out for the fraction of necrosis which represents the death of cells in living tissue. Because the aim of this study is to destroy the all tumor region in living tissue, i.e., necrosis region, mesh optimization is conducted for the fraction of necrosis. Typical fraction of necrosis at three different points (A, B, C) is given for five different mesh numbers in Table 3 for Case 5 at the end of eight minute. Points A, B and C are at 4 mm, 12 mm and 20 mm from center of probe, and they are shown in Figure 4b. It is seen that the fraction of necrosis does not change significantly when the mesh number changes from 176929 to 743265. Thus, mesh number of 290887 is chosen for the optimum mesh number, and this mesh number is used for the remaining calculations for Case 5. Similar mesh optimization analysis is performed when case is changed.

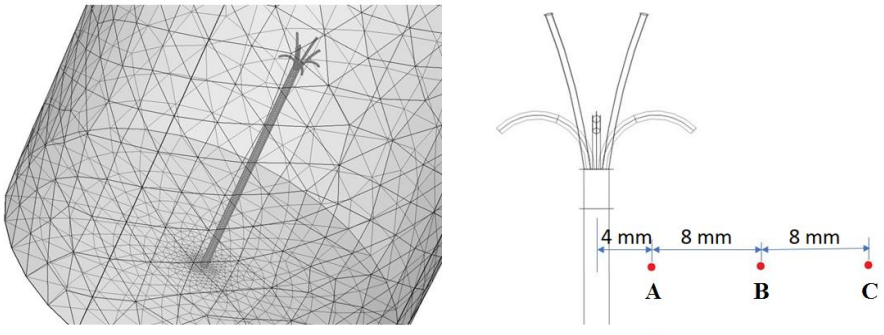

(a) (b)

Figure 4. (a) Typical mesh distribution and (b) points used to measure the fraction of necrosis.

Table 3. Fraction of necrosis according to number of mesh elements at three different points at the end of eight minute.

Points on Tissue	127874 elements	139853 elements	176929 elements	290887 elements	743265 elements
Point A	1	1	1	1	1
Point B	0.4	0.3	0.332	0.329	0.327
Point C	0.173	0.168	0.163	0.163	0.162

RESULTS

Numerical validation can be done with the results of Tungjitkusolmun et al. (2002), Chen et al. (2009) and Duan et al. (2016). Literature review showed that Tungjitkusolmun et al. (2002) is an accepted article which is highly cited by other researchers. Therefore, Tungjitkusolmun et al. (2002) has been the reason for preference to use it for literature comparison. The study of Tungjitkusolmun et al. (2002) was repeated here to show the accuracy of this numerical study. Three-dimensional finite element analysis for radiofrequency hepatic tumor ablation using four array umbrella-typed electrode was used. Temperature distribution of present study is shown in Figure 5a after eight minute of ablation. Figure 5b shows the temperature regions above than or equal to 50°C. The figure of Tungjitkusolmun et al. (2002) is not given here due to copyright (Please see Figures 4c and 4d in Tungjitkusolmun et al. (2002)). It is seen that the results of present study are in good agreement with the results of Tungjitkusolmun et al. (2002).

After verifying the accuracy of the numerical model, simulations are performed for five cases given in Figure 2. Lesion volumes obtained for Case 1 through Case 5 are seen in Figure 6 after eight minute. Gray area represents regions above than or equal to 50°C. It is seen that the shape of the lesion for Case 1 through Case 4 is nearly similar. It is also seen that the shape of the lesion is nearly spherical for Case 5, i.e., hybrid electrode.

After seeing that spherical lesion is obtained for Case 5 with four Christmas-tree and four umbrella-shaped electrodes, the numerical studies are conducted for Case 5. Evolution of lesion of Case 5 by the end of first, second, fourth, and eight minutes of ablation is seen in Figure 7. As can be seen from Figure 7, the shape is almost a sphere at the last minute, i.e., eight minute, of ablation. It is seen that the shape of lesion changes with time significantly until the end of four minute. However, results show that lesion shape almost remains the same when the time is changed from 4 to 8 minute.

Typical temperature distribution of Case 5 at the end of second, fourth, sixth, and eight minutes is shown in Figure 8. As can be seen in Figure 8, maximum temperature in tissue increases when the time increases. After eight minute of ablation, maximum temperature reaches to 94.2ºC. Because of the fact that temperature is less than 100ºC, tissue carbonization does not occur within the lesion (Tatli et al., 2012).

In order to see the dimensions of the lesion after the eight minute of ablation, the views of the lesion on *x*-*y* and *y*-*z* coordinates are shown in Figure 9. The diameter of the lesion obtained by hybrid design, i.e. Case 5, is approximately 20 mm which is suitable for small-medium tumors. This result agrees with the result of Rossi et al. (1990). It is seen that the shape of the lesion is nearly spherical.

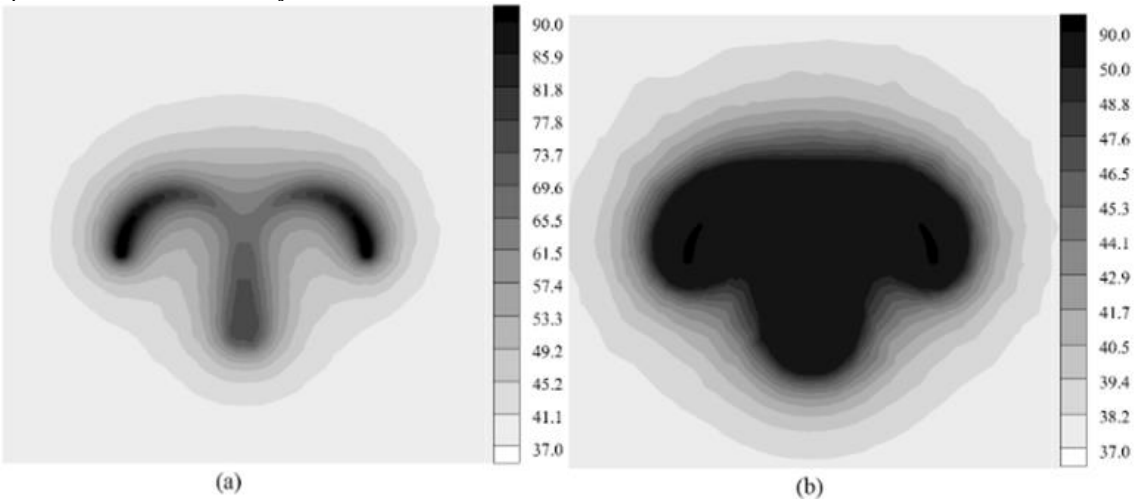

Figure 5. (a) Temperature distribution after eight minute of ablation, and (b) regions greater than or equal to temperature of 50°C.

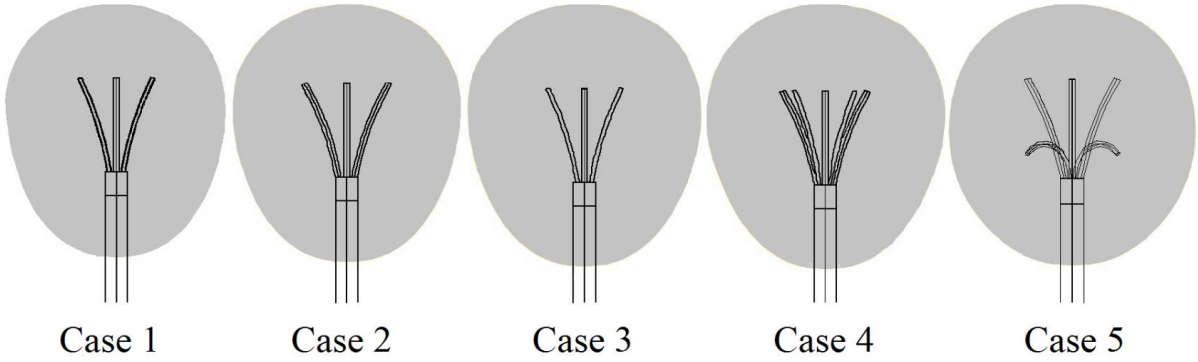

Figure 6. Lesion volumes after eight minute.

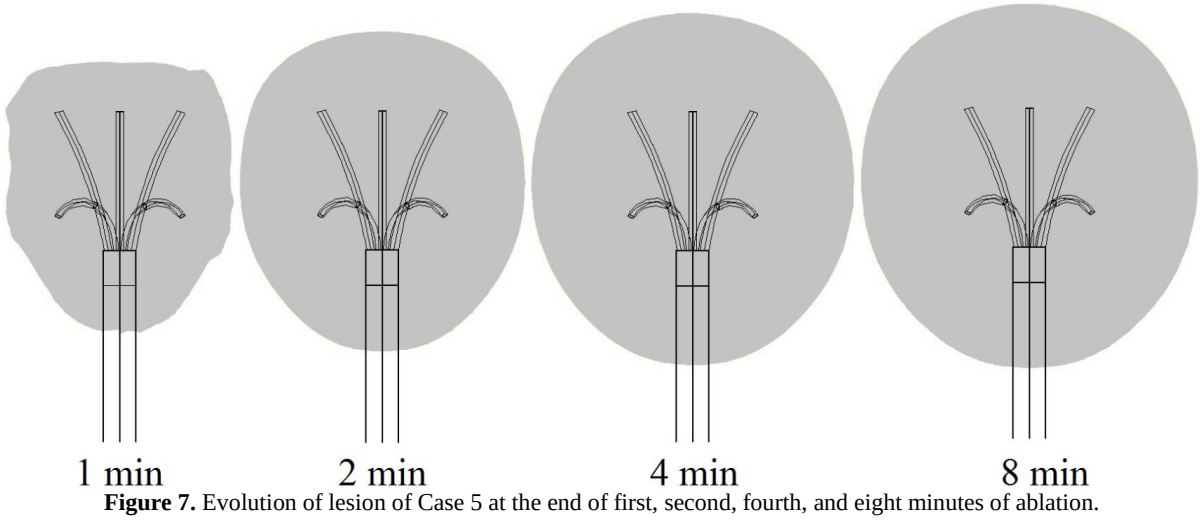

Figure 7. Evolution of lesion of Case 5 at the end of first, second, fourth, and eight minutes of ablation.

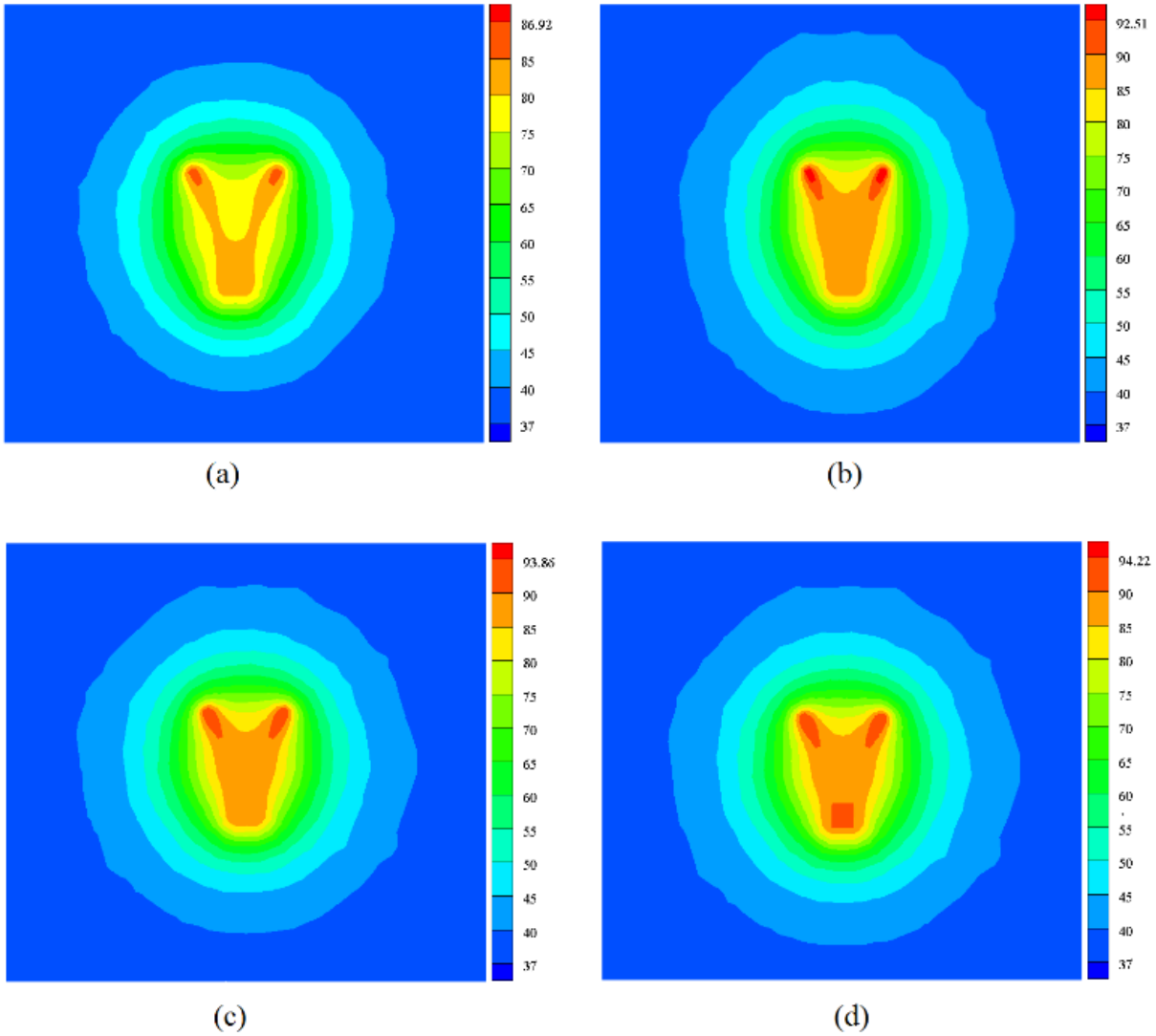

Figure 8. Typical temperature distribution of Case 5 at the end of first (a), second (b), fourth (c), and eight (d) minutes.

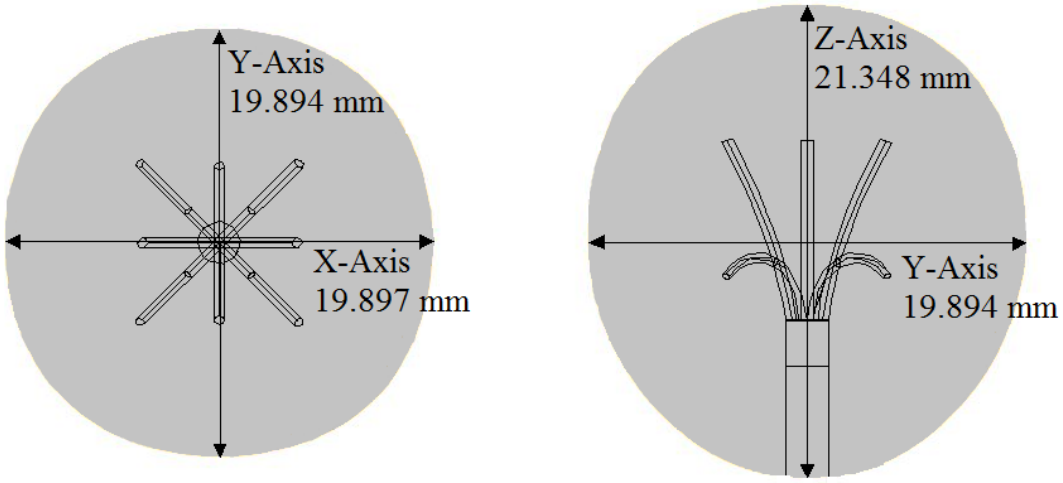

Figure 9. Dimensions of lesion after eight minute of ablation for Case 5.

CONCLUSION

A spherical-shaped lesion is obtained using a hybrid electrode for liver tissue. Three-dimensional finite element method is used. The COMSOL Multiphysics software is employed to simulate the problem. Electrical voltage, ablation time, geometry and number of electrodes are the investigated parameters. Results are presented in the form of lesion volume and temperature distribution. It is seen that present results are in good agreement with the literature results. Hybrid electrode construction consists of four Christmas-tree and four umbrella-shaped electrodes. It is seen that approximately 20 mm-diameter of lesion can be destroyed using hybrid electrode design after eight minutes. Results show that maximum temperature within tissue reaches to 94.2^{o}C after eight minutes of ablation. Spherical lesion is obtained for electrical voltage 30V and at the end of ablation time 8 minute. It is hoped that the hybrid electrode configuration can be used for treatment of spherical shape hepatic tumors in clinical applications.

REFERENCES

Ahmad M. I. M., 2016, Radiofrequency Ablation with Monopolar Cluster Versus Bipolar Multipolar Electrodes for the Ablation of ⩾2.5 cm Hepatocellular Carcinoma, *Egypt. J. Radiol. Nucl. Med*., 47, 1443-1449.

Audigier C., Mansi T., Delingette H., Rapaka S., Mihalef V., Carnegie D., Boctor E., Choti M., Kamen A., Ayache N. and Comaniciu D., 2015, Efficient Lattice Boltzmann Solver for Patient-Specific Radiofrequency Ablation of Hepatic Tumors, *IEEE T. Med. Imaging*, 34, 1576-1589.

Barajas M. S., Fraga T. C., Acevedo M. A. E. and Cabrera R. G., 2018, Radiofrequency Ablation: A Review of Current Knowledge, Therapeutic Perspectives, Complications, and Contraindication, *Int. J. Biosen. Bioelectron*, 4, 63-65.

Cartier V., Boursier J., Lebigot J., Oberti F., Fouchard-Hubert F. and Aubé C., 2016, Radiofrequency Ablation of Hepatocellular Carcinoma: Mono or Multipolar, *J. Gastroenterol. Hepatol.*, 31, 654-660.

Chang I. A. and Nguyen U. D., 2004, Thermal Modeling of Lesion Growth with Radiofrequency Ablation Devices, *Biomed. Eng.* 3, 1-19.

Chen C. C. R., Miga M. I. and Galloway R. L., 2009, Optimizing Electrode Placement Using Finite-Element Models in Radiofrequency Ablation Treatment Planning, *IEEE T. Bio-Med. Eng.*, 56, 237-245.

Choi J. W., Lee J. M., Lee D. H., Yoon J. H., Suh K. S., Yoon J. H., Kim Y. J., Lee J. H., Yu S. J. and Han J. K., 2016, Switching Monopolar Radiofrequency Ablation Using a Separable Cluster Electrode in Patients with Hepatocellular Carcinoma: A Prospective Study, *PLoS One*, 11, 1-17.

Clinical Practice Guidelines, 2012a, EASL-EORTC Clinical Practice Guidelines: Management of Hepatocellular Carcinoma, *Eur. J. Cancer*, 48, 599-641.

Clinical Practice Guidelines, 2012b, EASL-EORTC Clinical Practice Guidelines: Management of Hepatocellular Carcinoma, *J. Hepatol.*, 56, 908-943.

Curley S. A., Davidson B. S., Fleming R. Y., Izzo F., Stephens L. C., Tinkey P. and Cromeens D., 1997, Laparoscopically Guided Bipolar Radiofrequency Ablation of Areas of Porcine Liver, *Surg. Endosc.*, 11, 729-733.

De Baere T., Denys A., Wood B. J., Lassau N., Kardache M., Vilgrain V., Menu Y. and Roche A., 2001, Radiofrequency Liver Ablation: Experimental Comparative Study of Water-Cooled Versus Expandable Systems, *Am. J. Roentgenol.*, 176, 187-192.

Duan B., Wen R., Fu Y., Chua K.J. and Chui C.K., 2016, Probabilistic Finite Element Method for Large Tumor Radiofrequency Ablation Simulation and Planning, *Med. Eng. Phys.*, 38, 1360–1368.

Ferenci P., Fried M., Labrecque D., Bruix J., Sherman M., Omata M., Heathcote J., Piratsivuth T., Kew M., Otegbayo J. A., Zheng S. S., Sarin S., Hamid S. S., Modawi S. B., Fleig W., Fedail S., Thomson A., Khan A., Malfertheiner P., Lau G., Carillo F. J., Krabshuis J. and Le Mair A., 2010, Hepatocellular Carcinoma (HCC): A Global Perspective, *J. Clin. Gastroenterol.*, 44, 239-245.

Givehchi S., Wong Y. H., Yeong C. H. and Abdullah B. J. J., 2018, Optimal Approach for Complete Liver Tumor Ablation Using Radiofrequency Ablation: A Simulation Study, *Minimally Invasive Therapy & Allied Technologies*, 27, 81-89.

Goldberg S. N., Gazelle G. S., Halpern E. F., Rittman W. J., Mueller P. R. and Rosenthal D. I., 1996, Radiofrequency Tissue Ablation: Importance of Local Temperature Along the Electrode Tip Exposure in Determining Lesion Size and Shape, *Acad. Radiol*. 3, 212-218.

Haemmerich D., Chachati L., Wright A. S., Mahvi D. M., Lee Jr. F. T. and Webster J. G., 2003a, Hepatic Radiofrequency Ablation with Internally Cooled Probes: Effect of Coolant Temperature on Lesion Size, *IEEE Trans. Biomed. Eng.*, 50, 493-500.

Haemmerich D., Wright A. W., Mahvi D. M., Lee Jr. F. T. and Webster J. G., 2003b, Hepatic Bipolar Radiofrequency Ablation Creates Coagulation Zones Close to Blood Vessels: A Finite Element Study, *Med. Biol. Eng. Comput.*, 41, 317-323.

Hansen P. D., Rogers S., Corless C. L., Swanstrom L. L. and Siperstien A. E., 1999, Radiofrequency Ablation Lesions in a Pig Liver Model, *J. Surg. Res.*, 87, 114-121.

Ito N., Pfeffer J., Isfort P., Penzkofer T., Kuhl C. K., Mahnken A. H., Schmitz-Rode T. and Bruners P., 2014, Bipolar Radiofrequency Ablation: Development of a New Expandable Device, Cardiovasc. *Intervent. Radiol.*, 37, 770-776.

Kilic D., Uysal C., Akdur A., Kayipmaz C., Tepeoglu M., and Boyvat F., 2015, Chest Wall Implantation Metastasis Caused by Percutaneous Radiofrequency Ablation for Hepatic Tumor, *Ann. Thorac. Surg.*, 99, 1078–1080.

Lee J. M, Han J. K., Kim S. H., Lee J. Y., Kim D. J., Lee M. W., Cho G. G., Han C. J. and Choi B. I., 2004, Saline-Enhanced Hepatic Radiofrequency Ablation Using a Perfused-Cooled Electrode: Comparison of Dual Probe Bipolar Mode with Monopolar and Single Probe Bipolar Modes, *Korean J. Radiol.*, 5, 121-127.

Lencioni R., Goletti O., Armillotta N., Paolicchi A., Moretti M., Cioni D., Donati F., Cicorelli A., Ricci S., Carrai M., Conte P. F., Cavina E. and Bartolozzi C., 1998, Radio-Frequency Thermal Ablation of Liver Metastases with a Cooled-Tip Electrode Needle: Results of a Pilot Clinical Trial, *Eur. Radiol.*, 8, 1205-1211.

Lin S. M. and Lin D. Y., 2003, Percutaneous Local Ablation Therapy in Small Hepatocellular Carcinoma, *Chang. Gung. Med. J*, 26, 308-314.

Livraghi T., Goldberg S. N., Lazzaroni S., Meloni F., Solbiati L. and Gazelle G. S., 1999, Small Hepatocellular Carcinoma: Treatment with Radio-Frequency Ablation Versus Ethanol Injection, *Radiology*, 210, 655-661.

Livraghi T., Goldberg S. N., Monti F., Bizzini A., Lazzaroni S., Meloni F., Pellicanò S., Solbiati L. and Gazelle G. S., 1997, Saline-Enhanced Radio-Frequency Tissue Ablation in the Treatment of Liver Metastases, *Radiology*, 202, 205-210.

Mazzaferro V., Llovet J. M., Miceli R., Bhoori S., Schiavo M., Mariani L., Camerini T., Roayaie S., Schwartz M. E., Grazi G. L., Adam R., Neuhaus P., Salizzoni M., Bruix J., Forner A., De Carlis L., Cillo U., Burroughs A. K., Troisi R., Rossi M., Gerunda G. E., Lerut J., Belghiti J., Boin I., Gugenheim J., Rochling F., Van Hoek B. and Majno P., 2009, Predicting Survival after Liver Transplantation in Patients with Hepatocellular Carcinoma Beyond the Milan Criteria: A Retrospective, Exploratory Analysis, *Lancet Oncol.*, 10, 35-43.

McGahan J. P., Browning P. D., Brock J. M. and Tesluk H., 1990, Hepatic Ablation Using Radiofrequency Electrocautery, *Invest. Radiol.*, 25, 267-270.

Mulier S., Miao Y., Mulier P., Dupas B., Pereira P., De Baere T., Lencioni R., Leveillee R., Marchal G., Michel L. and Ni Y., 2005, Electrodes and Multiple Electrode Systems for Radio Frequency Ablation: A Proposal for Updated Terminology, *Adv. Exp. Med. Biol.*, 15, 798-808.

Ozbek O., Keskin F., Kaya H. E., Guler I., Nayman A., and Koc O., 2016, Radiofrequency Ablation of A Rare Pathology: Vertebral Intraosseous Lipoma, *Spine J.*, 16, e155

Poon D., Anderson B. O., Chen L. T., Tanaka K., Lau W. Y., Van Cutsem E., Singh H., Chow W. C., Ooi L. L., Chow P., Khin M. W. and Koo W. H., 2009, Management of Hepatocellular Carcinoma in Asia: Consensus Statement from the Asian Oncology Summit 2009, *Lancet Oncol.*, 10, 1111-1118.

Rossi S., Buscarini E., Garbagnati F., Di Stasi M., Quaretti P., Rago M., Zangrandi A., Andreola S., Silverman D. and Buscarini L., 1998, Percutaneous

Treatment of Small Hepatic Tumors by an Expendable RF Needle Electrode, *Am. J. Roentgenol.*, 170, 1015-1022.

Rossi S., Fornari F., Pathies C. and Buscarini L., 1990, Thermal Lesion Induced by 480 kHz Localized Current Field in Guinea Pig and Pig Liver, *Tumori*, 76, 54-57.

Shao Y. L., Arjun B., Leo H. L. and Chua K. J., 2017, Nano-Assisted Radiofrequency Ablation of Clinically Extracted Irregularly-Shaped Liver Tumors, *J. Therm. Biol.*, 66, 101–113.

Stippel D. L., Brochhagen H. G., Arenja M., Hunkemöller J., Hölscher A. H. and Beckurts K. T., 2004, Variability of Size and Shape of Necrosis Induced by Radiofrequency Ablation in Human Livers: A Volumetric Evaluation, *Annals of Surgical Oncology*, 11, 420–425.

Tatli S., Tapan U., Morrison P. R. and Silverman S. G., 2012, Radiofrequency Ablation: Technique and Clinical Applications, Diagn. *Interv. Radiol.*, 18, 508-516.
Tungjitkusolmun S., Staelin S.T., Haemmerich D., Tsai J. Z., Cao H. Webster J. G., Lee F. T., Mahvi D. M. and Vorperian V. R., 2002, Three-Dimensional Finite-Element Analyses for Radio-Frequency Hepatic Tumor Ablation. *IEEE Trans. Biomed. Eng.*, 49, 3-9.

Verslype C., Rosmorduc O. and Rougier P., 2012, Hepatocellular Carcinoma: ESMO-ESDO Clinical Practice Guidelines for Diagnosis, Treatment and Follow-up. *Ann. Oncol.*, 23, 41-48.

Yang L., Wen R., Qin J., Chui C. K., Lim K. B. and Chang S., 2010, A Robotic System for Overlapping Radiofrequency Ablation in Large Tumor Treatment, *IEEE/ASME Trans. Mechatron.*, 15, 887-897.